

MEASUREMENT OF THE RADIATIVE COOLING RATE FOR KRYPTON AND ARGON AND THEIR PROFILES IN THE FTU PLASMA

D. Pacella, **B.C. Gregory**¹, L. Gabellieri, G. Mazzitelli, M. Leigheb, G. Pizzicaroli,
K.B. Fournier², W.H. Goldstein², M. May³ and M. Finkenthal³

Associazione EURATOM-ENEA sulla Fusione, Frascati, Rome, Italy

¹*INRS-Energie et Matériaux and CCFM, Varennes, Québec, Canada*

²*Lawrence Livermore National Laboratory, Livermore, CA 94550, USA*

³*The Johns Hopkins University, Baltimore, MD 21218, USA*

1. Introduction

The radiative cooling curves of krypton and argon, along with the temporal evolution of their density profiles, were measured in the FTU plasma by injection of fairly substantial quantities of these gases into standard discharges. The technique involved the inversion of chordal profiles of visible Bremsstrahlung and bolometry, and depends upon the fact that the intrinsic impurities, mainly molybdenum, remained constant.

2. Method

The plasma conditions were as follows: $B_T = 6T$, $I_p = 500\text{ kA}$, $\langle n_e \rangle = 5.10^{19}\text{ m}^{-3}$, $R_o = 0.94\text{ m}$, $a = 0.29\text{ m}$. These impurities were injected at 0.5-0.6 s during the discharge plateau from a valve on the outside of plasma and took 30-50 ms before substantially penetrating the discharge. At a chosen time, the 11 chords of the vertical Bremsstrahlung camera were inverted using a routine [1] employing the Zerniche polynomial technique. The accuracy of the routine was carefully checked in tests using inversions of known analytical radial functions.

From the definition of Z_{eff} we obtain the following relationships before gas injection (primed symbols) and during injection (no primes). Krypton is used as an example in the following.

$$(1) \quad n_e(r)' Z_{\text{eff}}(r)' = n_d(r)' + \sum_i^N n_i(r)' Z_i^2(r)'$$

$$(2) \quad n_e(r) Z_{\text{eff}}(r) = n_d(r) + n_{\text{Kr}}(r) Z_{\text{Kr}}^2(r) + \sum_i^N n_i(r) Z_i^2(r)$$

The symbols are all functions of minor radius, r . Spectroscopic measurements show that intrinsic impurity levels remain constant at all times considered. Subtracting the two equations gives an expression for the argon or krypton density:

$$(3) \quad n_{\text{Kr}}(r) Z_{\text{Kr}}^2(r) = n_e(r) Z_{\text{eff}}(r) - n_e(r)' Z_{\text{eff}}(r)' .$$

The visible free-free Bremsstrahlung emission, e_{ff} [$\text{W}\cdot\text{m}^{-3}\cdot\text{sr}^{-1}\cdot\text{nm}^{-1}$] is related to the effective charge state, Z_{eff} , by the equation [2]:

$$(4) \quad Z_{\text{eff}} = K \frac{e_{\text{ff}} \lambda^2 \sqrt{T_e}}{n_e^2 g_{\text{ff}} \exp\left[-\frac{1240}{\lambda T_e}\right]}, \quad \text{with } g_{\text{ff}} = \frac{\sqrt{3}}{\pi} \ln\left[\frac{4 e^{-g} \lambda T_e}{1240}\right]$$

where $K = 6.67 \times 10^{35}$, λ = wavelength in nm, n_e = electron density in m^{-3} , T_e = electron temperature in eV, and $g = 0.5772$ is Euler's constant. Equations (3) and (4) are combined to give the krypton or argon density:

$$(5) \quad n_{\text{Kr}}(r) = \frac{4.1 \times 10^{24}}{Z_{\text{Kr}}^2(r)} \left\{ \frac{e_{\text{ff}}(r) \sqrt{T_e(r)} \exp\left[\frac{2.3 \times 10^{-3}}{T_e(r)}\right]}{n_e(r) \ln[978 T_e(r)]} - \frac{e_{\text{ff}}(r)' \sqrt{T_e(r)'} \exp\left[\frac{2.3 \times 10^{-3}}{T_e(r)'}\right]}{n_e(r)' \ln[978 T_e(r)']} \right\} \text{m}^{-3}$$

where now T_e is in keV, $\lambda = 540$ nm and the emissivities, e_{ff} , are in $\text{photons}\cdot\text{s}^{-1}\cdot\text{m}^{-3}\cdot\text{sr}^{-1}\cdot\text{nm}^{-1}$.

This expression is evaluated at different times to determine $n_{\text{Ar}}(r,t)$ and $n_{\text{Kr}}(r,t)$. The Z_{Kr}^2 curves are taken from reference [3], assuming that transport effects do not alter these curves significantly. T_e and n_e are measured respectively using electron cyclotron emission corrected by Thomson scattering and a far infrared laser interferometer.

A similar technique is applied to the 13 channel bolometry camera. Before injection of the artificial impurity the radiated power is

$$(6) \quad P_r(r)' = \sum_i^N n_i(r)' Q_i[T_e(r)'] n_e(r)'$$

and during injection

$$(7) \quad P_r(r) = n_{\text{Kr}}(r) Q_{\text{Kr}}(T_e) n_e(r) + \sum_i^N n_i(r) Q_i(T_e) n_e(r) .$$

Here P_r' and P_r are the radiated power densities, n_i' and n_i are the intrinsic impurity densities, n_{Kr} is the Kr or Ar density, Q_{Kr} is the radiative cooling rate for the injected gas, and Q_i is the same quantity for the intrinsic impurities. Primed quantities are before injection. We subtract equations (6) and (7), assuming similar quantities of intrinsic impurities, and that $Q_i(T_e') = Q_i(T_e)$, a reasonably good approximation since the temperature decreases only by 10-

20% during injection. An expression for the cooling rate of Kr or Ar in terms of the radiated power, the injected impurity density, and the electron density is easily obtained as follows:

$$(8) \quad Q_{Kr}[T_e(r)] = \frac{1}{n_{Kr}(r)} \left[\frac{P_r(r)}{n_e(r)} - \frac{P_r(r)'}{n_e(r)'} \right]$$

We have verified that for the densities given by equation (5) at different times, equation (8) gives the same Q values, as expected.

3. Results

Figures 1 and 2 give the krypton and argon density profiles as a function of minor radius in the outer half of the plasma. The radial coordinate is referenced to the geometric plasma centre and the inversion routine takes into account the Shafranov shift which is not negligible in FTU. The krypton density profile, measured during the gas inflow where the increase of the central flat region is quite linear and fast, results flat in the central region ($r/a \leq 0.5$) and rises sharply toward the edge, out to where the analysis technique is no longer valid. Argon, on the contrary, is measured in a later phase when its density is approaching a steady-state value. Its density has rather flat profiles, increasing much more slowly in time.

The cooling curves obtained from equation (8) are shown in Fig. 3 and 4 for krypton and argon along with the ADPAK [3] curves and very recent *ab initio* calculations labelled HULLAC [4], developed at Lawrence Livermore N.L. Results show that for krypton the measured radiation bump is roughly a factor of 2 lower than the ADPAK value and much broader, in agreement with the HULLAC curve, but is displaced toward higher temperatures. The argon cooling curve gives a radiation barrier of about the same height and at the same temperature as ADPAK, somewhat higher than HULLAC, but broader in shape toward higher temperatures. It is thought

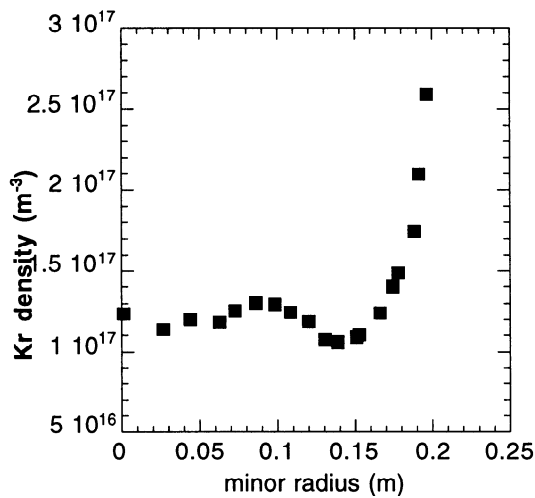


Fig. 1 - Krypton density profile (# 13730 $t=1.4s$)

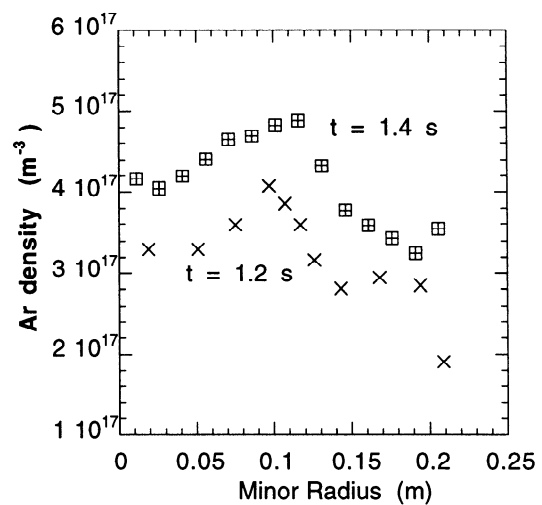


Fig. 2 - Argon density profile (#13640)

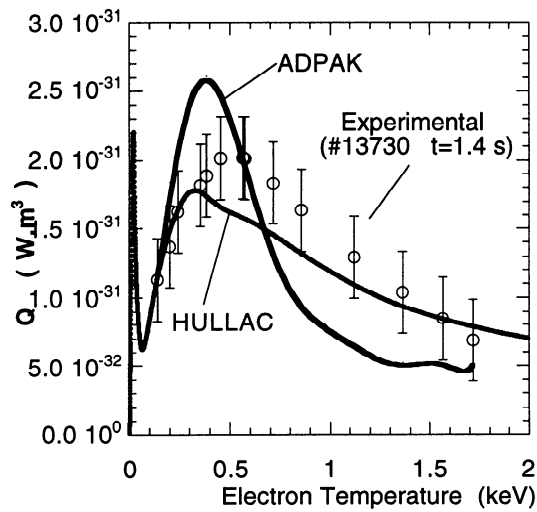


Fig. 3 - Cooling curve for Krypton

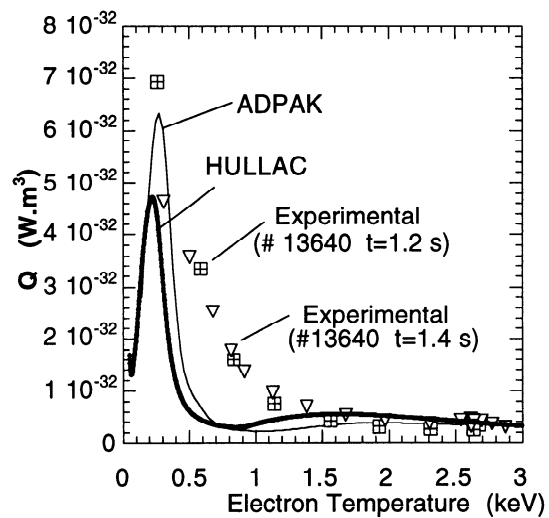


Fig. 4 - Cooling curve for Argon

that some of this broadening may be due to the inversion technique and/or transport effects. A portion of the present work was performed under the auspices of the U.S Department of Energy by the Lawrence Livermore National Laboratories under contract No. W-7405-ENG-48.

4. References

- [1] F. Alladio, P. Micozzi, *Nucl. Fusion*, **35**, 305 (Appendix B) 1995.
- [2] K. Kadota et al., *Nucl. Fusion*, **20**, 209 (1980).
- [3] D.E. Post et al., *Atomic Data and Nuclear Data Tables*, **20**, 397 (1977).
- [4] K.B. Fournier et al. "Calculated Radiative Power Losses from Mid- and High-Z Impurities in tokamak plasmas", 11th Topical Conference, AIP Woodbury, NY (1998).